Fluctuation and Noise Letters
Vol. 3, No. 2 (2003) L195–L204

World Scientific
www.worldscientific.com

NOISE-INDUCED PHASE SYNCHRONIZATION: THEORETICAL AND EXPERIMENTAL RESULTS

JAN A. FREUND
Institut für Physik, Humboldt-Universität Berlin
Invalidenstr. 110, D-10115 Berlin, Germany
freund@physik.hu-berlin.de

SYLVAIN BARBAY
Laboratoire de Photonique et de Nanostructures
CNRS - UPR 20, Route de Nozay 91460 Marcoussis, France

STEFANO LEPRI
Dip. di Energetica, Via S. Marta 3, 50139 Firenze, Italy
and INFM, UdR Firenze, Italy

ALESSANDRO ZAVATTA
Dip. di Sistemi e Informatica, Via S. Marta 3, 50139 Firenze, Italy

GIOVANNI GIACOMELLI
Istituto Nazionale di Ottica Applicata
Largo E. Fermi 6, 50125 Firenze, Italy,
and INFM, UdR Firenze, Italy
giacomelli@inoa.it

Received 11 December 2002
Revised 2 April 2003
Accepted 3 April 2003

The beneficial role fluctuations can play in the process of phase synchronization is analyzed in terms of a model with binary input and output signals. Special attention is paid to the relation between noise-induced phase synchronization and the well-known phenomenon of stochastic resonance. Analytic predictions are compared with experimental data from a vertical cavity surface emitting laser. Various measures for aperiodic stochastic resonance, frequency entrainment and stochastic phase synchronization reveal a satisfactory agreement between theory and experiment.

Keywords: Frequency entrainment; locking episodes; aperiodic stochastic resonance; dichotomic signals; VCSEL; alternating polarization configurations.

1. Introduction

In parallel to the big boom of chaos synchronization [1,2] frequency and phase synchronization in stochastic systems [3] have repeatedly received considerable interest. Several decades after the seminal works of Stratonovich [4], the revival of effective phase synchronization explains from the discovery that, for sufficiently strong albeit subthreshold input signals, the phenomenon of stochastic resonance (SR) [5, 6] can be reinterpreted in terms of a noise-induced phase synchronization (NIPS). Shortly after its first experimental and numerical observation [7,8] the relation between aperiodic SR [9, 10] and NIPS with stochastic signals [11] was established. Eventually, a fully analytical description of NIPS was reported [12,13] that was based on binary input and output signals. A direct application of the theory was given in the context of behavioural biology [14]. Recent experiments with a vertical cavity surface emitting laser (VCSEL) [15] that investigated the stochastic switchings between alternating polarization configurations under the influence of a stochastic binary input signal and noise were analyzed in the context of binary aperiodic SR [16, 17].

In this paper we present a comparison of the quantifiers for NIPS, extracted from the last-mentioned VCSEL data, with related analytic expressions from the theory. To this end, we first discuss different definitions of phase synchronization in Sec. 2. A short outline of the analytic approach with resulting expressions for the relevant NIPS measures is sketched in Sec. 3. The comparison between experiment and theory presented in Sec. 4 constitutes the core of our publication. Conclusions and an outlook close this Letter.

2. Definitions of Phase Synchronization

Different definitions of phase synchronization exist with implications for its measurement:

1. In the purely deterministic case two systems with instantaneous phases $\phi_1(t)$ and $\phi_2(t)$ are locked (in the $n : m$ mode) if a suitably defined phase difference $\varphi_{n,m}(t) = n\phi_1(t) - m\phi_2(t)$ remains bounded for all times. For weak external periodic forcing of an autonomous oscillator the dynamics of the instantaneous phase difference ($\varphi = \varphi_{1,1}$) is governed by the Adler equation [18]

$$\dot{\varphi} = \Delta - \Delta_s \cos\varphi \tag{1}$$

that can be identified with the overdamped motion of a particle in a tilted and corrugated potential $U(\varphi) = -\Delta\varphi + \Delta_s \sin\varphi$ (see Fig. 1). The transition from the locked to the running solution occurs when the ratio of the frequency mismatch (or detuning) Δ and the synchronization bandwidth (parameter of nonlinearity) Δ_s exceeds unity, i.e.,

$$\left|\frac{\Delta}{\Delta_s}\right| \begin{cases} < 1 \text{ locked solution,} \\ > 1 \text{ running solution.} \end{cases} \tag{2}$$

2. In the presence of unbounded fluctuations, as they occur, for instance, in Gaussian noise, even in the locked situation $|\Delta| < \Delta_s$ the phase difference will

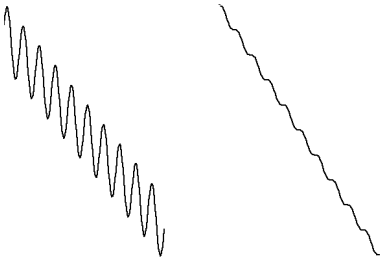

Fig. 1. The transition from the locked solution (left) to the running solution (right) occurs when the modulus of the frequency mismatch (Δ) exceeds the synchronization bandwidth (Δ_s).

not remain bounded for all times. Sufficiently large fluctuations eventually will cause phase slips. The noisy dynamics of the phase difference is described by the stochastic Adler equation [19]

$$\dot{\varphi} = \Delta - \Delta_s \cos\varphi + \sqrt{2D}\xi(t) \tag{3}$$

that is now related to the Brownian motion of a particle in the same tilted and corrugated potential $U(\varphi) = -\Delta\varphi + \Delta_s \sin\varphi$. An ensemble of systems prepared with a narrow peaked initial distribution of phases, as shown in the top panel of Fig. 2, will evolve in time such that the distribution drifts and disperses in the way sketched in the bottom panel of Fig. 2.

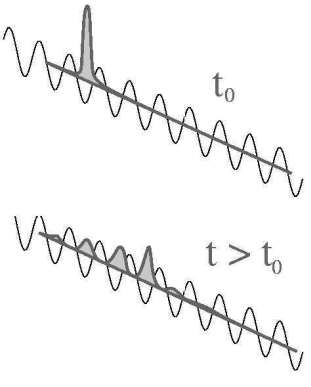

Fig. 2. An ensemble with a narrow initial distribution will evolve in time due to fluctuations that cause phase slips. The net effect can be described in terms of phase drift and phase diffusion.

The time T between phase slips is a stochastic variable. In case its average $\langle T_{\rm lock}\rangle$ is large in comparison with the typical time scale T_0 of the external drive, e.g. its period, it is justified to regard the situation as effectively phase locked and to consider $\langle T_{\rm lock}\rangle$ as the average duration of locking episodes. To quantify $\langle T_{\rm lock}\rangle$ we consider the second moment of the phase difference

$$\langle\varphi^2\rangle = \langle\omega\rangle^2\langle T_{\rm lock}\rangle^2 + 2\mathcal{D}_{\rm eff}\langle T_{\rm lock}\rangle = \pi^2 \tag{4}$$

that combines the drift, specified by the average frequency $\langle\omega\rangle$, and the diffusion, determined by the effective phase diffusion coefficient $\mathcal{D}_{\rm eff}$. Identifying

the second moment with π^2 defines a phase slip and yields the quadratic equation (4) that can be readily solved for $\langle T_{\rm lock}\rangle$. In this way we can quantify the criterion for effective phase synchronization as

$$\frac{\langle T_{\rm lock}\rangle}{T_0} = \frac{\mathcal{D}_{\rm eff}}{\langle\omega\rangle^2 T_0}\left[\sqrt{1+\left(\frac{\pi\langle\omega\rangle}{\mathcal{D}_{\rm eff}}\right)^2}-1\right] \gg 1\,. \tag{5}$$

Deriving expressions for the drift or diffusion dominated regimes [13] underlines that effective phase synchronization requires both drift *and* diffusion of the phase difference to be sufficiently small. Moreover, this immediately implies that frequency locking ($\langle\omega\rangle$ small) without phase locking ($\mathcal{D}_{\rm eff}$ large) can occur.

3. There exists a definition of phase synchronization in the statistical sense that relates to the deviation of the wrapped phase distribution [4] from an equidistribution. This definition is widely used in the neurosciences and medical applications [20]. We want to point out that this is a much weaker definition than that based on the average duration of locking episodes (5). To underline this statement we point out that for large subthreshold signals and low noise levels the rare threshold crossing events will be mainly concentrated around the maxima of the signal. We will, thus, find a sharply peaked distribution of the wrapped phase difference for suboptimal noise intensity, i.e., even outside the regime of SR.

4. The phenomenon of SR is often discussed in terms of a noise-induced *synchronized* hopping between the two wells of a driven bistable potential [5]. Several measures for periodic SR, e.g. the signal-to-noise ratio, the spectral power amplification or the residence-time distribution, and for aperiodic SR, e.g. correlation coefficients, coherence function or information theoretic measures, are used to pinpoint the effect. It is important to notice that SR already can be observed in the linear response regime [5], i.e. for arbitrary small signal amplitudes, whereas NIPS sets in only beyond some minimal signal amplitudes [12]. From this we conclude that all measures proving SR in the linear response regime *cannot* be measures of NIPS.

3. Analytic Predictions

In this section we briefly outline the approach that culminates in explicit expressions for $\langle\omega\rangle$ and $\mathcal{D}_{\rm eff}$ and, thus, allows to evaluate our preferred criterion (5) for NIPS analytically. As mentioned before, the approach is based on dichotomic signal representations for the input $(-1,+1)$ and the output $(-1,+1)$ of a stochastic resonator and as such optimally fits the experimental results of the VCSEL experiment [16, 17]. In this twice dichotomic signal representation the drive-response system is described in terms of four states that are connected by transitions as shown in Fig. 3.

While the switching rate γ of the assumed dichotomic Markovian input is uniform the output switching events depend on the instantaneous configuration and

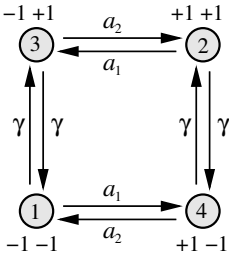

Fig. 3. Schematic diagram of the twice dichotomic stochastic system: vertical transitions correspond to a switch of the input whereas horizontal transitions indicate a flip of the output state. For a dichotomic Markovian input switches occur with a constant rate γ. The two noise dependent rates a_1 and a_2 characterize the switching behaviour of the resonator and involve the amplitude A of the driving signal in such a way ($a_1 < a_2$) that the asynchronous states (3 and 4) are depopulated in favour of the synchronous ones (1 and 2).

are governed by the two noise dependent rates

$$a_1 = \alpha(D) \exp\left(-\frac{A}{D}\right) \quad \text{and} \quad a_2 = \alpha(D) \exp\left(+\frac{A}{D}\right) \tag{6}$$

where

$$\alpha(D) = \alpha_\infty \exp\left(-\frac{\Delta V}{D}\right) \tag{7}$$

is the Kramers rate of the symmetric stochastic resonator, i.e. for vanishing input signal ($\alpha(D) = a_1 = a_2$ for $A = 0$). From (6) we see that with increasing input amplitude A the growing imbalance $a_2 - a_1 \geq 0$ is responsible for depopulating the asynchronous states (3 and 4) in favour of the synchronous ones (1 and 2). Of course, we always obey $A < \Delta V$ to keep the input signal subthreshold.

Due to the restriction of twice dichotomic signals related phases $\phi_{\rm in}(t)$ and $\phi_{\rm out}(t)$ are discrete, viz. multiples of π, and the same is true for the instantaneous phase difference $\varphi(t) = k(t)\pi$. Being equipped with the rates γ, a_1 and a_2 we can formulate the stochastic dynamics of the phase difference by virtue of a master equation

$$\frac{\partial P_{\rm k}}{\partial t} = \gamma\,(P_{\rm k+1} - P_{\rm k}) + g_{\rm k-1}P_{\rm k-1} - g_{\rm k}P_{\rm k} \tag{8}$$

where $P_{\rm k}$ is a shorthand notation for $P(\varphi = k\pi, t|\varphi_0, t_0)$, i.e., the probability to experience a value $k\pi$ for the phase difference φ at time t (conditioned by some initial value φ_0 at time t_0), and

$$g_{\rm k} = \alpha(D)\, \exp\left(-\cos(k\pi)\frac{A}{D}\right). \tag{9}$$

Note that $\sigma(\varphi) = \cos(\varphi)$ is the normalized[a] input-output correlator, hence, $\langle\sigma\rangle$ is nothing but the standard correlation coefficient widely used as a key quantifier for aperiodic SR [9, 11]. It is straightforward to derive a kinetic equation for this

[a]By restriction to the binary values ± 1 the standard deviations of input and output signals are one.

quantity from the master equation and, subsequently, its asymptotic stationary value

$$\langle \sigma^* \rangle = \frac{a_2 - a_1}{2\gamma + a_1 + a_2}\,. \tag{10}$$

A similar treatment yields the average frequency

$$\langle \omega \rangle = \langle \dot{\varphi} \rangle = -\langle \omega_{\rm in} \rangle + \langle \omega_{\rm out} \rangle = \pi \left[-\gamma + \frac{a_1 + a_2}{2} - \frac{a_2 - a_1}{2} \langle \cos \varphi \rangle \right] \tag{11}$$

with a related stationary asymptotic expression $\langle \omega^* \rangle$ by substituting $\langle \sigma^* \rangle$ for $\langle \cos \varphi \rangle$. Notice that (11) resembles the averaged stochastic Adler equation (3); in this context we identify $\pi[\frac{a_1+a_2}{2} - \gamma]$ with the frequency mismatch Δ and $\pi \frac{a_2-a_1}{2}$ with the synchronization bandwidth Δ_s. The noise dependence of both these parameters is the very reason why noise-induced frequency locking can occur.

In Fig. 4 (right panel) we plot the stationary switching frequency of the output $\langle \omega^*_{out} \rangle / \pi = \langle \omega^* \rangle / \pi + \gamma$ as a function of the noise intensity D for various subthreshold amplitudes A (the values of all parameters are specified in Sec.4). For sufficiently large amplitudes we find a plateau of the curve at the switching frequency of the input. This is a clear signature of noise-induced frequency locking and the first prerequisite of NIPS.

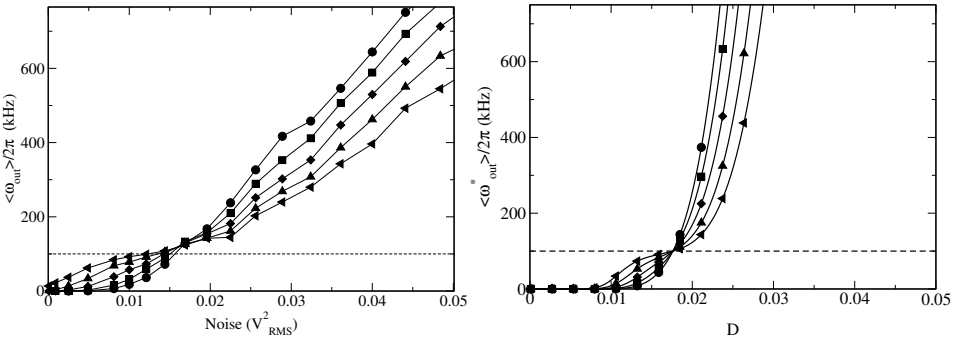

Fig. 4. Average output switching frequency $\langle \omega_{\rm out} \rangle$ vs. noise intensity D for a binary input signal (with bit duration $T_b = 2.5\mu$s) and for increasing driving amplitudes (left experiment $A_{\rm exp}$, right model $A = \eta \Delta V$): circles - 50 mV and $\eta = 0.08$, boxes - 100 mV and $\eta = 0.16$, diamonds - 150 mV and $\eta = 0.24$, triangles up - 200 mV and $\eta = 0.32$, triangles left - 250 mV and $\eta = 0.4$; other parameters see text. The horizontal dashed lines mark $\gamma/2 = 100$ kHz.

A calculation of the effective diffusion coefficient $\mathcal{D}_{\rm eff}$ proceeds by computing the following expression

$$\mathcal{D}_{\rm eff} = \frac{1}{2} \partial_t [\langle \varphi^2 \rangle - \langle \varphi \rangle^2]\,. \tag{12}$$

The calculation is straightforward and since it is published in [12] we will not show the explicit result here. The basic structure of the asymptotic stationary expression is $\mathcal{D}_{\rm eff} = \mathcal{D}_{\rm in} + \mathcal{D}_{\rm out} - \mathcal{D}_{\rm co}$ with obvious interpretation of $\mathcal{D}_{\rm in} = \gamma \pi^2/2$ and $\mathcal{D}_{\rm out} = \langle \omega^* \rangle \pi/2$. The coherence term $\mathcal{D}_{\rm co}$ alone can cause a diminishing of the effective phase diffusion. Since it combines terms that all scale with powers of the stationary

input-output correlator $\langle \sigma^* \rangle$ a high value of the latter is necessary. In Fig. 5 (right panel) we show the stationary effective diffusion coefficient $\mathcal{D}^*_{\rm eff}$ as a function of noise intensity D for the same set of parameters chosen in Fig. 4. In the zero-noise limit phase diffusion is solely due to the stochastic input signal and, thus, attains the value $\mathcal{D}_{\rm in} = \gamma\pi^2/2$. For sufficiently large amplitudes we see that the diffusion is reduced below this value if the strength of fluctuations is chosen optimally; this is the second prerequisite of NIPS.

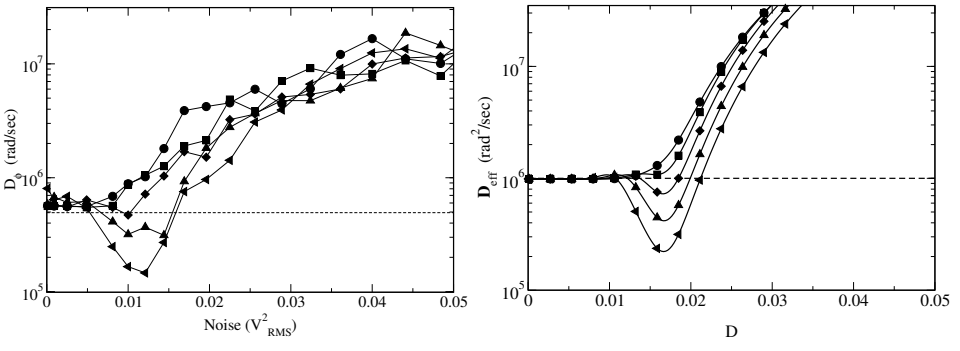

Fig. 5. Stationary effective diffusion coefficients $\mathcal{D}^*_{\rm eff}$ of the phase difference φ vs. noise intensity D and for the driving amplitudes of Fig. 4 (left experiment, right model). The horizontal dashed lines mark the expected zero noise values (see text): left $\gamma\frac{\pi^2}{4} \approx 500$ rad^2 kHz; right $\gamma\frac{\pi^2}{2} \approx 1000$ rad^2 kHz.

Being equipped with both $\langle \omega \rangle$ and $\mathcal{D}_{\rm eff}$ (for the stationary asymptotics) we can readily compute the average duration of locking episodes according to the expression in (5). The result is shown in Fig. 6 (right panel). With increasing signal amplitude a narrow peak occurs for optimal noise that, for the largest amplitude, indicates a mean locking duration of four to five switches of the input.

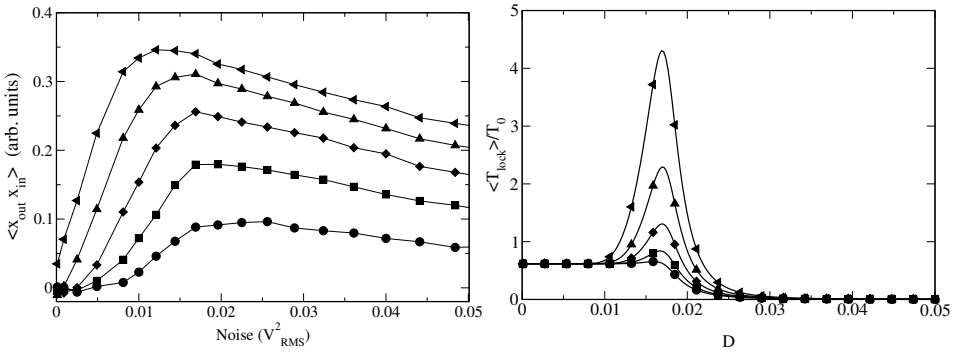

Fig. 6. Left: the experimental input-output correlator $\langle x_{\rm out} x_{\rm in} \rangle$ (non-normalized) vs. noise intensity D and for the driving amplitudes of Fig. 4. Right: the theoretical average duration of locking episodes $\langle T_{\rm lock} \rangle$ (normalized to the mean input switching time $T_0 = \gamma^{-1}$) vs. noise. Notice that the correlator maintains large values even in the region of high noise intensities where phase slips occur rather frequently, thus limiting the duration of locking epochs.

4. Comparison Between Experiment and Theory

The physical system is composed of a VCSEL followed by a polarizer and a detection system (see Ref. [15] for a detailed description of the setup). By sweeping the pump current, the laser can emit in different polarization and transverse profile configurations. The transition between two states is generally characterized by a bistable current region, where noise-induced jumps occur between the two states. In this case the laser dynamics can be reproduced by a van't Hoff-Arrhenius process, with average residence times usually given by a Kramers law, i.e., an exponential function of the inverse noise intensity [21]. By feeding in additional noise into the pump current, the statistics of the jumps can thus be changed. The polarization fluctuations are transformed into light intensity variations by the polarizer and detected by means of a photodiode whose signal is acquired by a digital scope. The signals from a variable intensity, white-noise generator (10 MHz bandwidth) and a pseudo-random binary sequence generator are summed and coupled into the laser input current. The current steps are chosen small enough not to induce a laser state jump without the aid of noise (subthreshold condition). The binary sequence is a 16,000-bit word with a bit duration denoted T_b [16, 17]. Even though the distribution of residence times $T_{\rm in}$ scales exponentially, i.e., $p(T_{\rm in} = k\,T_b) = 2^{-k}$, its coefficient of variation (the ratio of standard deviation and mean) is $1/\sqrt{2}$ which is slightly at variance with the value one for the dichotomic Markovian process used in the theory.

An example of the signal detected by the photodiode, for different values of the input noise strength, is shown in Fig. 7. For low noise (Fig. 7(a)) the laser mainly remains in its initial state, even if a small amplitude modulation is visible. Increasing the noise, some jumps occur (Fig. 7(b)) and, for an input noise around 400 mV_{rms}, the output closely follows the input signal (Fig. 7(c)). Finally, for larger noise strengths, the laser dynamics is determined by the fluctuations rather than by the input string, with a strong decorrelation between input and output (Fig. 7(d),(e)).

To describe the data of the VCSEL measurements the parameters of the model, i.e., α_∞, ΔV, A and D have to be related to the control parameters of the experiment. Some relations between experimental and model parameters were discussed in [15–17] and used to estimate $\alpha_\infty = 1$ Ghz. For the effective barrier height we chose $\Delta V = 0.15$ (in units that are identically used for D). The subthreshold signal amplitude is related to the barrier height via $A = \eta \Delta V$ with $0 \leq \eta < 1$. A linear relation between the experimental signal amplitudes $A_{\rm exp}$ and the model parameter A was fitted such that $A_{\rm exp} = 250$ mV corresponds to $\eta = 0.4$.

The study of the NIPS regime in the experiment can be carried out by evaluating both the average frequency (Fig. 4) and the effective diffusion coefficient (Fig. 5) from the measured laser time series. We used different methods for the definition of the phase difference, namely, the Hilbert transform and the linearly interpolated phase [3]. Both definitions gave the same results. The direct comparison of experimental results with analytic data shows a satisfactory qualitative agreement. The discrepancies between experimental and theoretical curves can be explained by the simplistic identification of the model parameter D with experimental noise intensity. In [15] (cf. Fig. 7 therein) intrinsic noise (zero offset) and saturation effects

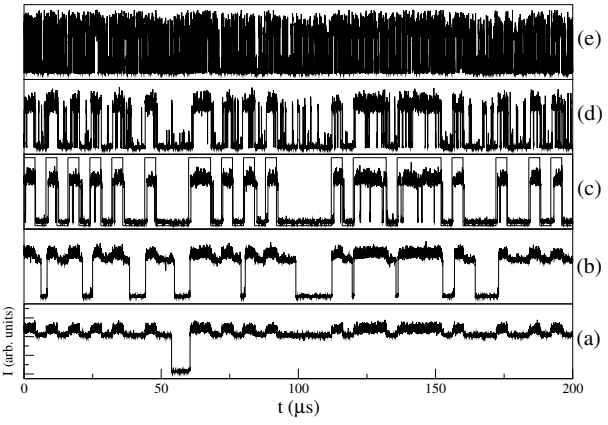

Fig. 7. Polarized laser intensity I for different input noise intensities, with a 50 MHz acquisition bandwidth. (a): 100, (b): 200, (c): 400, (d): 600 and (e): 1200 mV_{rms}. In (c) the input pattern is shown (with an arbitrary vertical scale). A sequence of 50 bits (bit duration: $T_b = 4\mu$s) is displayed.

(nonlinear stretching for large noise) were shown to exist when fitting experimental data to a phenomenological bistable model. A closer analysis of these relations in the context of the analytic model is left to future research. Moreover, the discrepancy of a factor two that is observed between the zero-noise phase diffusion coefficients of experiment and theory follows directly from the aforementioned difference in the coefficients of variation of the input switch time distributions.

Returning to our statements about the difference between measures for SR and NIPS we also present the experimental input-output correlator $\langle x_{\mathrm{out}} x_{\mathrm{in}} \rangle$ in Fig. 6 (left panel) together with the average duration of locking episodes $\langle T_{\mathrm{lock}} \rangle$ according to (5) (right panel). As can be seen from the figure the rapid uprise of $\langle x_{\mathrm{out}} x_{\mathrm{in}} \rangle$ marks the onset of NIPS, however, the correlator is still high in a region beyond optimal noise where the average locking episodes are already rather short. This discrepancy between the quantifiers pinpoints the difference between (aperiodic) SR and NIPS.

5. Conclusions

The phenomenon of NIPS is a much more stringent effect than (aperiodic) SR. For noise intensities where SR occurs NIPS may or may not occur. Specific NIPS measures are based on the average duration of locking episodes. Experimental data of the VCSEL driven by a binary stochastic input (similar to a dichotomic Markovian process) were evaluated proving the occurrence of NIPS in a narrow range of noise intensities outside of which the correlation between input and output is still significant. Based on a semi-quantitative analysis, i.e., some parameters were derived from measurement data while others were fitted, the experimental measures of NIPS can be reproduced to some extent by analytic expressions from a simple stochastic four state model. To obtain a better quantitative agreement a more careful analysis of the relation between experimental and model parameters is required.

References

[1] H. Fujisaka and Y. Yamada, *Stability theory of synchronized motion in coupled-oscillator systems*, *Prog. Theor. Phys.* **69** (1983) 32–47.

[2] L. Pecora and T. Carroll, *Synchronization in chaotic systems*, *Phys. Rev. Lett.* **64** (1990) 821–824.

[3] J. A. Freund, L. Schimansky-Geier and P. Hänggi, *Frequency and phase synchronization in stochastic systems*, *Chaos* **13** (2003) 225–238.

[4] R. L. Stratonovich, *Topics in the Theory of Random Noise*, Gordon and Breach, New York (1967).

[5] L. Gammaitoni, P. Hänggi, P. Jung and F. Marchesoni, *Stochastic resonance*, *Rev. Mod. Phys.* **70** (1998) 223–287.

[6] V. S. Anishchenko, A. B. Neiman, F. Moss and L. Schimansky-Geier, *Stochastic resonance: noise-enhanced order*, *Phys. Usp.* **42** (1999) 7–36.

[7] B. Shulgin, A. Neiman and V. Anishchenko, *Mean switching frequency locking in stochastic bistable systems driven by a periodic force*, *Phys. Rev. Lett.* **75** (1995) 4157–4160.

[8] A. Neiman, A. Silchenko, V. Anishchenko and L. Schimansky-Geier, *Stochastic resonance*: *noise-enhanced phase coherence*, *Phys. Rev. E* **58** (1998) 7118–7125.

[9] J. J. Collins, C. C. Chow and T. T. Imhoff, *Aperiodic stochastic resonance in excitable systems*, *Phys. Rev. E* **52** (1995) R3321–R3324.

[10] A. Neiman, L. Schimanmsky-Geier and F. Moss, *Linear response theory applied to stochastic resonance in models of ensembles of oscillators*, *Phys. Rev. E* **56** (1997) R9–R12.

[11] A. Neiman, L. Schimansky-Geier, F. Moss, B. Shulgin and J. J. Collins, *Synchronization of noisy systems by stochastic signals*, *Phys. Rev. E* **60** (1999) 284–292.

[12] J. A. Freund, A. B. Neiman and L. Schimansky-Geier, *Analytic description of noise-induced phase synchronization*, *Europhys. Lett.* **50** (2000) 8–14.

[13] J. A. Freund, A. B. Neiman and L. Schimansky-Geier, *Stochastic resonance and noise-induced phase coherence*, in P. Imkeller and J. von Storch, eds. *Stochastic Climate Models. Progress in Probability*, Boston, Basel (Birkhäuser, 2001), pages 309–323.

[14] J. A. Freund, J. Kienert, L. Schimansky-Geier, A. Neiman, D. F. Russell, T. Yakusheva and F. Moss, *Behavioral stochastic resonance*: *how a noisy army betrays its outpost*, *Phys. Rev. E* **63** (2000) 031910.

[15] S. Barbay, G. Giacomelli and F. Marin, *Stochastic resonance in vertical cavity surface emitting lasers*, *Phys. Rev. E* **61** (2000) 157–166.

[16] S. Barbay, G. Giacomelli and F. Marin, *Experimental evidence of binary aperiodic stochastic resonance*, *Phys. Rev. Lett.* **85** (2000) 4652–4655.

[17] S. Barbay, G. Giacomelli and F. Marin, *Noise-assisted transmission of binary information*: *theory and experiment*, *Phys. Rev. E* **63** (2001) 051110–1–9, 2001.

[18] R. Adler, *A study of locking phenomena in oscillators*, *Proc. IRE* **34** (1946) 351–357.

[19] P. Hänggi and P. Riseborough, *Dynamics of nonlinear dissipative oscillators*, *Am. J. Phys.* **51** (1983) 347–352.

[20] P. Tass, M. G. Rosenblum, J. Weule, J. Kurths, A. Pikovsky, J. Volkmann, A. Schnitzler and H.-J. Freund, *Detection of n*: *m* phase locking from noisy data: *application to magnetoencephalography*, *Phys. Rev. Lett.* **81** (1998) 3291–3294.

[21] P. Hänggi, P. Talkner and M. Borkovec, *Reaction-rate theory*: *fifty years after karmers*, *Rev. Mod. Phys.* **62** (1990) 251–341.